Cell Reports, Volume *31*

Supplemental Information

Genome-wide Profiling Identifies DNA Methylation Signatures of Aging in Rod Photoreceptors Associated with Alterations in Energy Metabolism

Ximena Corso-Díaz, James Gentry, Ryan Rebernick, Catherine Jaeger, Matthew J. Brooks, Freekje van Asten, Keshav Kooragayala, Linn Gieser, Jacob Nellissery, Raul Covian, Tiziana Cogliati, Anupam K. Mondal, Ke Jiang, and Anand Swaroop

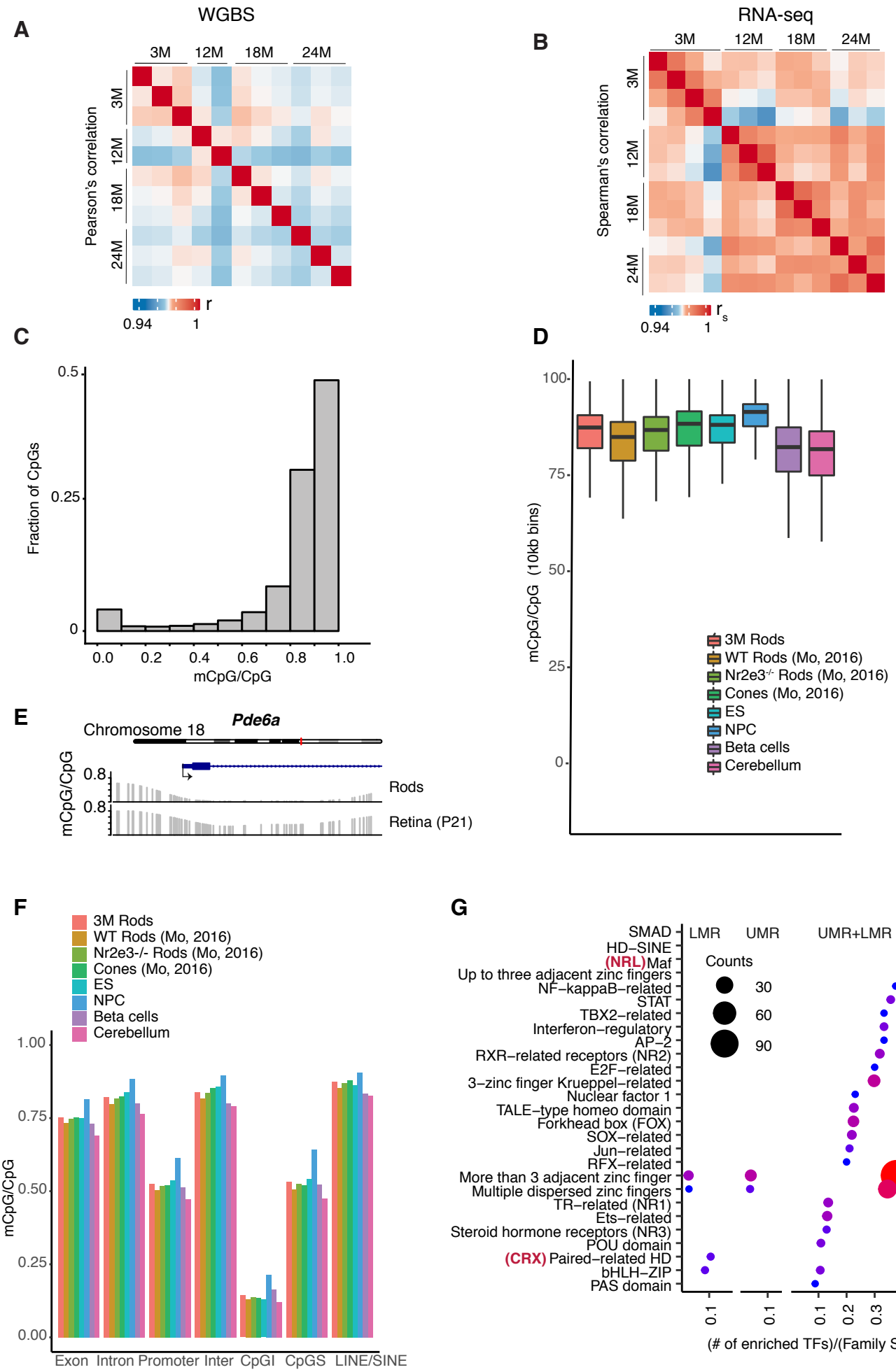
A
WGBS
3M
12M
18M
24M
Pearson's correlation
r
0.94
1
B
RNA-seq
Spearman's correlation
r_s
C
Fraction of CpGs
mCpG/CpG
D
mCpG/CpG (10kb bins)
3M Rods
WT Rods (Mo, 2016)
Nr2e3-/- Rods (Mo, 2016)
Cones (Mo, 2016)
ES
NPC
Beta cells
Cerebellum
E
Chromosome 18
Pde6a
mCpG/CpG
Rods
Retina (P21)
F
mCpG/CpG
Exon
Intron
Promoter
Inter
CpGI
CpGS
LINE/SINE
G
LMR
UMR
UMR+LMR
Counts
SMAD
HD-SINE
(NRL) Maf
Up to three adjacent zinc fingers
NF-kappaB-related
STAT
TBX2-related
Interferon-regulatory
AP-2
RXR-related receptors (NR2)
E2F-related
3-zinc finger Krueppel-related
Nuclear factor 1
TALE-type homeo domain
Forkhead box (FOX)
SOX-related
Jun-related
RFX-related
More than 3 adjacent zinc finger
Multiple dispersed zinc fingers
TR-related (NR1)
Ets-related
Steroid hormone receptors (NR3)
POU domain
(CRX) Paired-related HD
bHLH-ZIP
PAS domain
(# of enriched TFs)/(Family Size)

Figure S1. Characteristics of the rod methylome and transcriptome. Related to figure 1. Correlation matrix of aging datasets based on A) DNA methylation and B) RNA expression. The heatmap shows the correlation coefficients (r, Pearson correlation; r_s, Spearman correlation) between whole-genome bisulfite sequencing (WGBS) or RNA-seq samples (WGBS: n = 3 for 3M, 18M, 24M; n = 2 for 12M; RNA-seq: n = 4 for 3M and n = 3 for 12M, 18M and 24M). C) Fraction of methylated CpGs genome-wide. D) Comparison of CpG methylation levels (mean over 10 kb bins) in different tissues and cell types. WT = wild type; ES = embryonic stem cell; NPC = neural precursor cell. The methylomes of wild-type rods, cones and *Nr2e3*$^{-/-}$ rods were obtained from (Mo, et al., 2016), NPC and ES from (Stadler et al., 2011), cerebellum from (Hon et al., 2013) and beta cells from (Avrahami et al., 2015). (E) Comparison of CpG methylation levels at the promoter region of *Pde6a* in purified rods obtained in this study and whole adult retina (P21) from a published dataset (Aldiri et al., 2017). Methylation levels were obtained using the same pipeline (see methods). F) CpG methylation levels at different genomic regions of various tissues and cell types. Inter = intergenic; CpGi = CpG island; CpGs = CpG shore. G) Transcription factor motifs identified in UMRs, LMRs or both regions using TRANSFAC (p-value < 0.05). Families that had at least 3 enriched transcription factors (TFs) are shown. The number of TF families represented in DMRs (counts) are depicted by the size of the dots (30 = blue, 60 = purple, 90 = red). Paired-related HD family includes CRX. Maf family includes NRL.

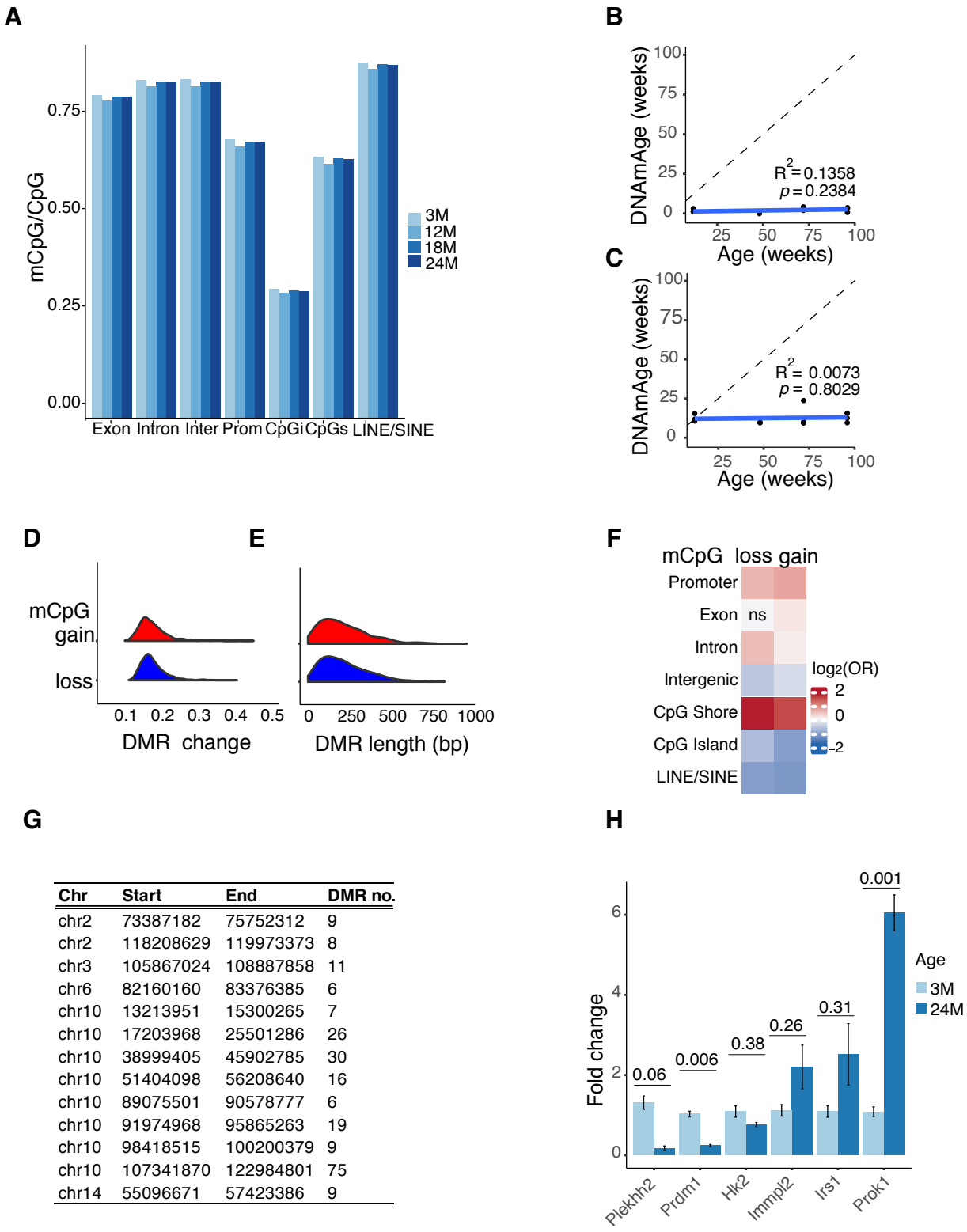

Chr	Start	End	DMR no.
chr2	73387182	75752312	9
chr2	118208629	119973373	8
chr3	105867024	108887858	11
chr6	82160160	83376385	6
chr10	13213951	15300265	7
chr10	17203968	25501286	26
chr10	38999405	45902785	30
chr10	51404098	56208640	16
chr10	89075501	90578777	6
chr10	91974968	95865263	19
chr10	98418515	100200379	9
chr10	107341870	122984801	75
chr14	55096671	57423386	9

Figure S2. DNA methylation differences across time-points. Related to figures 2 and 5. A) Mean CpG methylation in different genomic regions at different time points. Inter = intergenic; prom = promoter; CpGi = CpG island; CpGs = CpG shore. B,C) Correlation between biological and epigenetic age using the B) (Stubbs et al., 2017) and C) (Meer et al., 2018) multi-tissue clocks. D,E) Distribution of DMRs by D) change difference and E) length in base pairs (bp). F) Heatmap showing the odds ratio (OR) of CpG counts within each genomic region. G) Table showing the location of DMR hotspots and DMR number per hotspot in rods. H) Bar graph showing the fold change expression difference by qRT-PCR of genes that harbor differential DNA methylation and expression by RNA-seq. Values were obtained using the delta-delta CT method normalized against *Hnrnpd*. DMR = differentially methylated region; n = 4 for 3M; n = 3 for 24M. Error bars, +/- SEM. Fold change means were compared between 3M and 24M using unpaired students t-test. *p* values are shown for each comparison.

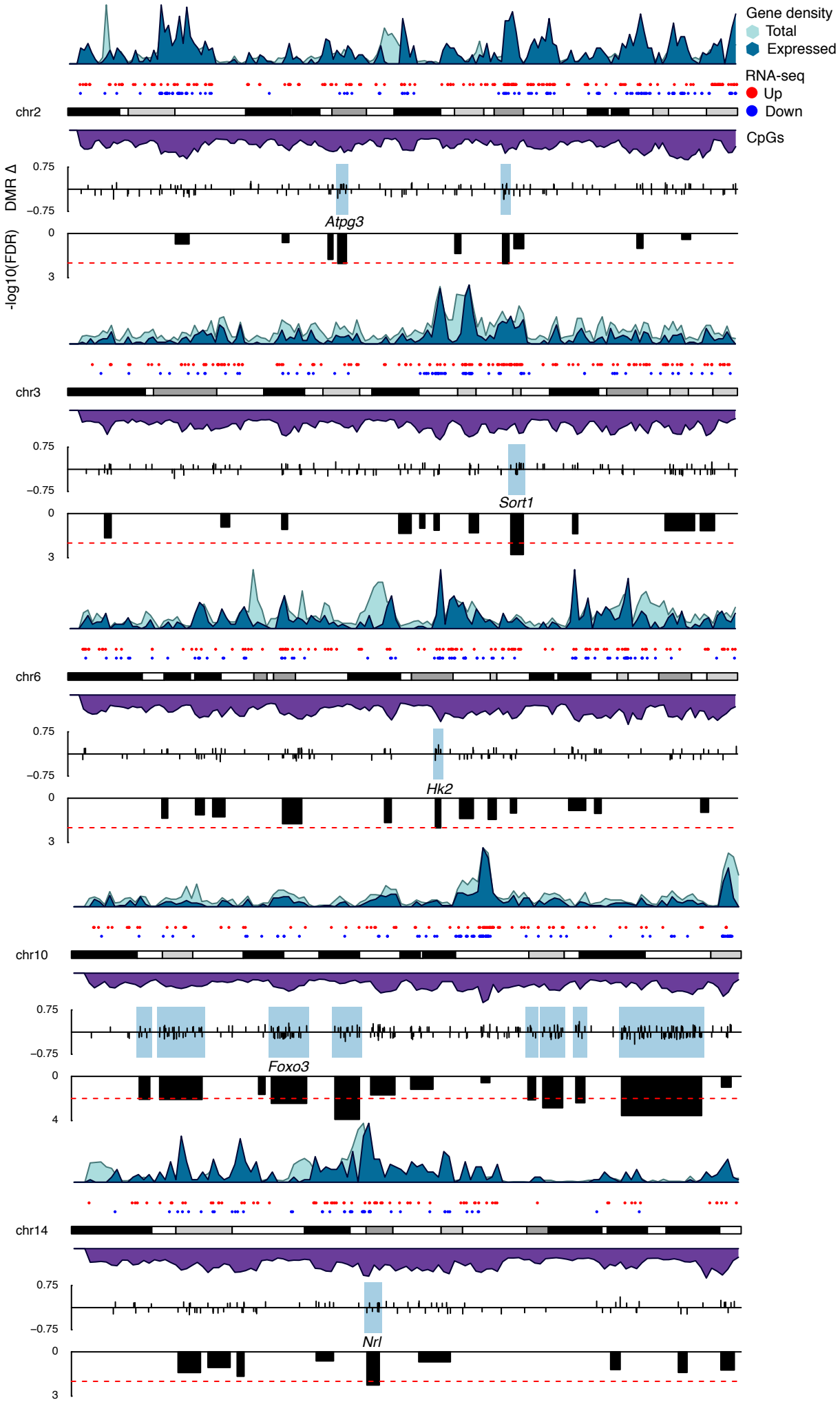
Gene density
Total
Expressed
RNA-seq
Up
Down
CpGs
chr2
DMR Δ
0.75
−0.75
-log10(FDR)
0
3
Atpg3
chr3
Sort1
chr6
Hk2
chr10
Foxo3
4
chr14
Nrl

Figure S3. Chromosomal DMR hotspots. Related to figure 2. Idiograms showing chromosomes 2, 3, 6,10 and 14 showing regions of DMR hotspots (blue boxes). DMRs that gain or lose methylation with age are shown as black ticks. DMR density higher than average, determined by a region-growing algorithm (see methods), is displayed in black boxes. Red dotted line indicates the *p*-value cutoff (FDR ≤ 0.01) of the hotspot enrichment after correcting for CpG number and gene density. On top, gene density is shown for all genes (light blue) and expressed genes > 10 CPM (darker blue). Upregulated and downregulated genes are shown in red and blue dots, respectively. CpG density is shown in purple. DMR = differentially methylated region.

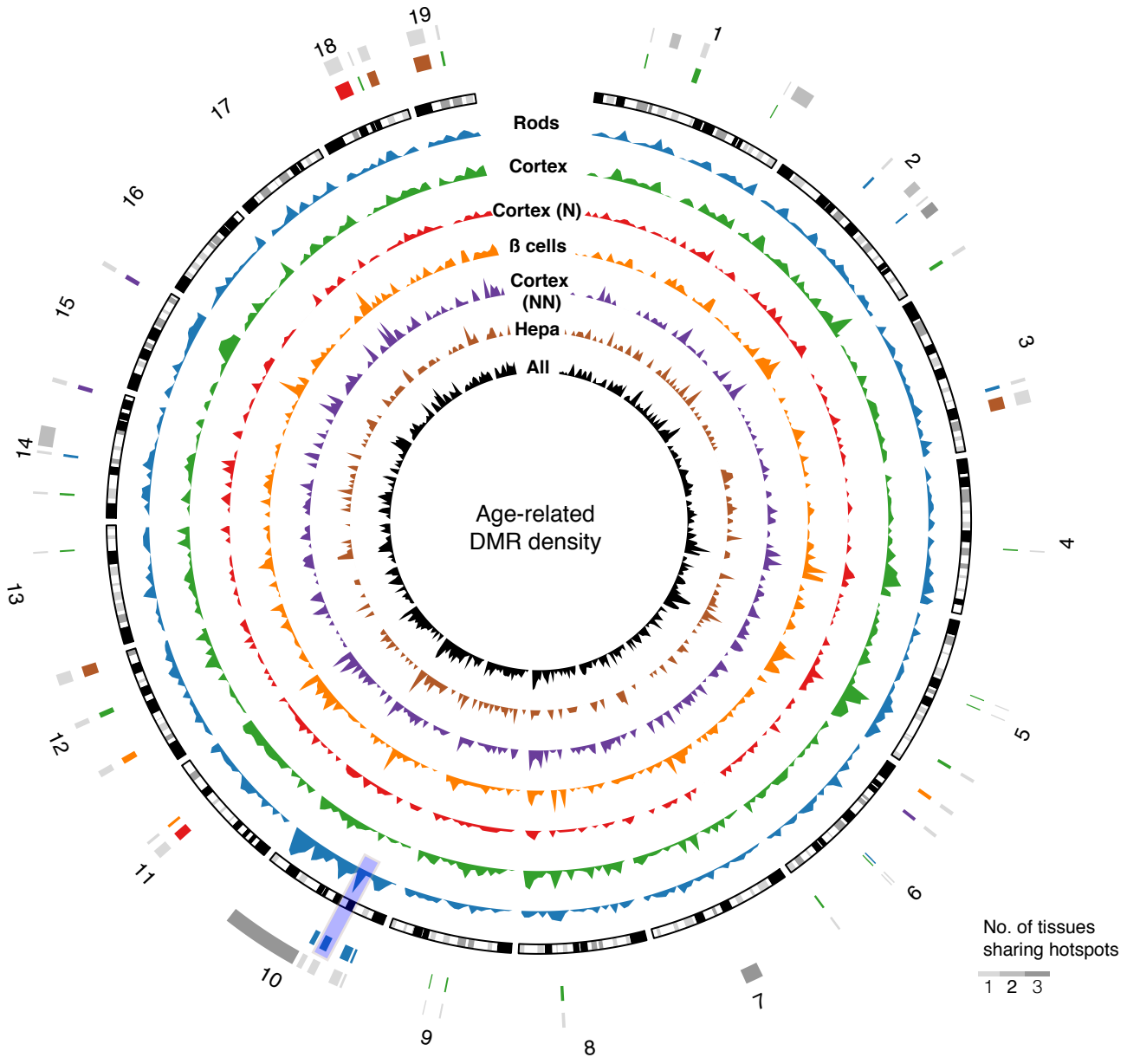

Figure S4. Distribution of DMR hotspots in various tissues. Related to figure 2. Circos plot showing DMR (differentially methylated region) hotspots (high age-associated DMR density, p -value ≤ 0.01) in rods (blue), whole frontal cortex (green), neuronal frontal cortex (N) (red), non-neuronal frontal cortex (NN) (purple) cells, beta cells (orange) and liver cells (Hepa) (brown). The combined densities are shown in black. The second outermost circle displays the location of unique hotspots for each tissue. Hotspots shared by more than one tissue are shown in the outermost circle. A hotspot located in a region reported to function as a longevity interactome is highlighted with a purple box.

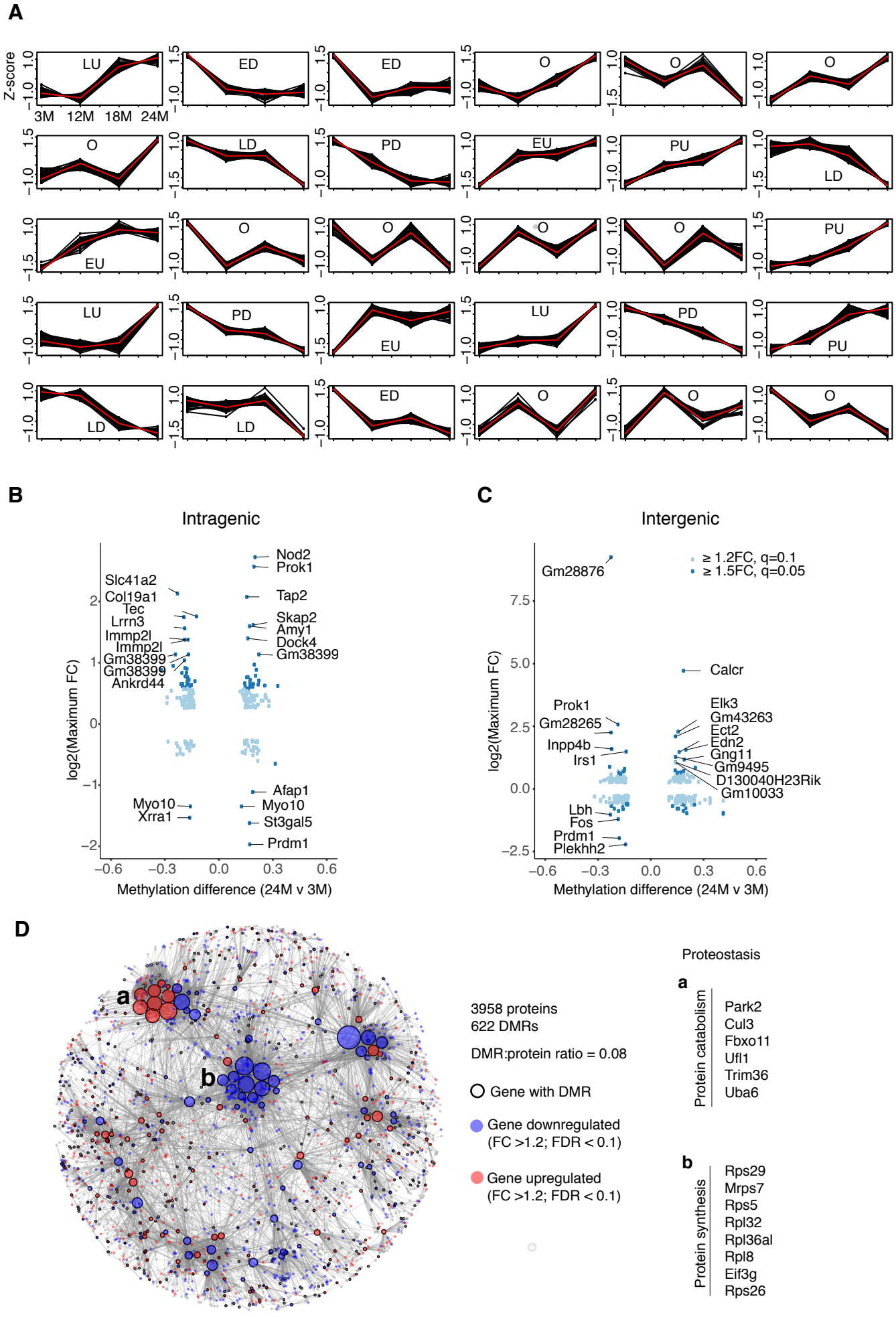
A
Z-score
3M 12M 18M 24M
LU
ED
ED
O
O
O
O
LD
PD
EU
PU
LD
EU
O
O
O
O
O
PU
LU
PD
EU
LU
PD
PU
LD
LD
ED
O
O
O
B
Intragenic
log2(Maximum FC)
Methylation difference (24M v 3M)
Nod2
Prok1
Slc41a2
Col19a1
Tec
Lrrn3
Tap2
Skap2
Amy1
Immp2l
Immp2l
Dock4
Gm38399
Gm38399
Gm38399
Ankrd44
Afap1
Myo10
Xrra1
Myo10
St3gal5
Prdm1
C
Intergenic
≥ 1.2FC, q=0.1
≥ 1.5FC, q=0.05
log2(Maximum FC)
Methylation difference (24M v 3M)
Gm28876
Calcr
Prok1
Gm28265
Inpp4b
Irs1
Elk3
Gm43263
Ect2
Edn2
Gng11
Gm9495
D130040H23Rik
Gm10033
Lbh
Fos
Prdm1
Plekhh2
D
a
b
3958 proteins
622 DMRs
DMR:protein ratio = 0.08
Gene with DMR
Gene downregulated
(FC >1.2; FDR < 0.1)
Gene upregulated
(FC >1.2; FDR < 0.1)
Proteostasis
a
Protein catabolism
Park2
Cul3
Fbxo11
Ufl1
Trim36
Uba6
b
Protein synthesis
Rps29
Mrps7
Rps5
Rpl32
Rpl36al
Rpl8
Eif3g
Rps26

Figure S5. Patterns of DMR progression. Related to figures 4 and 5. A) Different patterns of DNA methylation changes were identified by unsupervised clustering (taking the negative squared distances of z-score values for each DMR). EU = early up; ED = early down; PU = progressive up; PD = progressive down; LU = late up; LD = late down; O = other patterns. B,C) Plot of differential methylation against gene expression fold change for B) intragenic and C) intergenic DMRs. Names of genes with top 10%-fold-changes are shown. Light blue = Absolute Fold-change (FC) $\geq$ 1.2, q-value $\leq$ 0.1; Dark blue = Absolute FC $\geq$ 1.5, q-value $\leq$ 0.05. D) First-degree protein-protein interaction network generated with 317 genes containing age-related DMRs and displaying differential gene expression. Only expressed genes were used. The network contains 3958 proteins, out of which, 622 are encoded by genes associated with DMRs. The DMR:protein ratio for the whole network is 0.08. The node size represents the number of interacting partners a protein has (see table S6 for information on the network node and edge list). Blue and red represent downregulated and upregulated genes respectively. Grey represents genes that do not change in expression. Genes with black borders have differential methylation. Note two main hubs in the network, “a” and “b”, associated with upregulation of protein degradation and downregulation of protein synthesis pathways, respectively. The names of proteins in hubs “a” and “b” are shown.

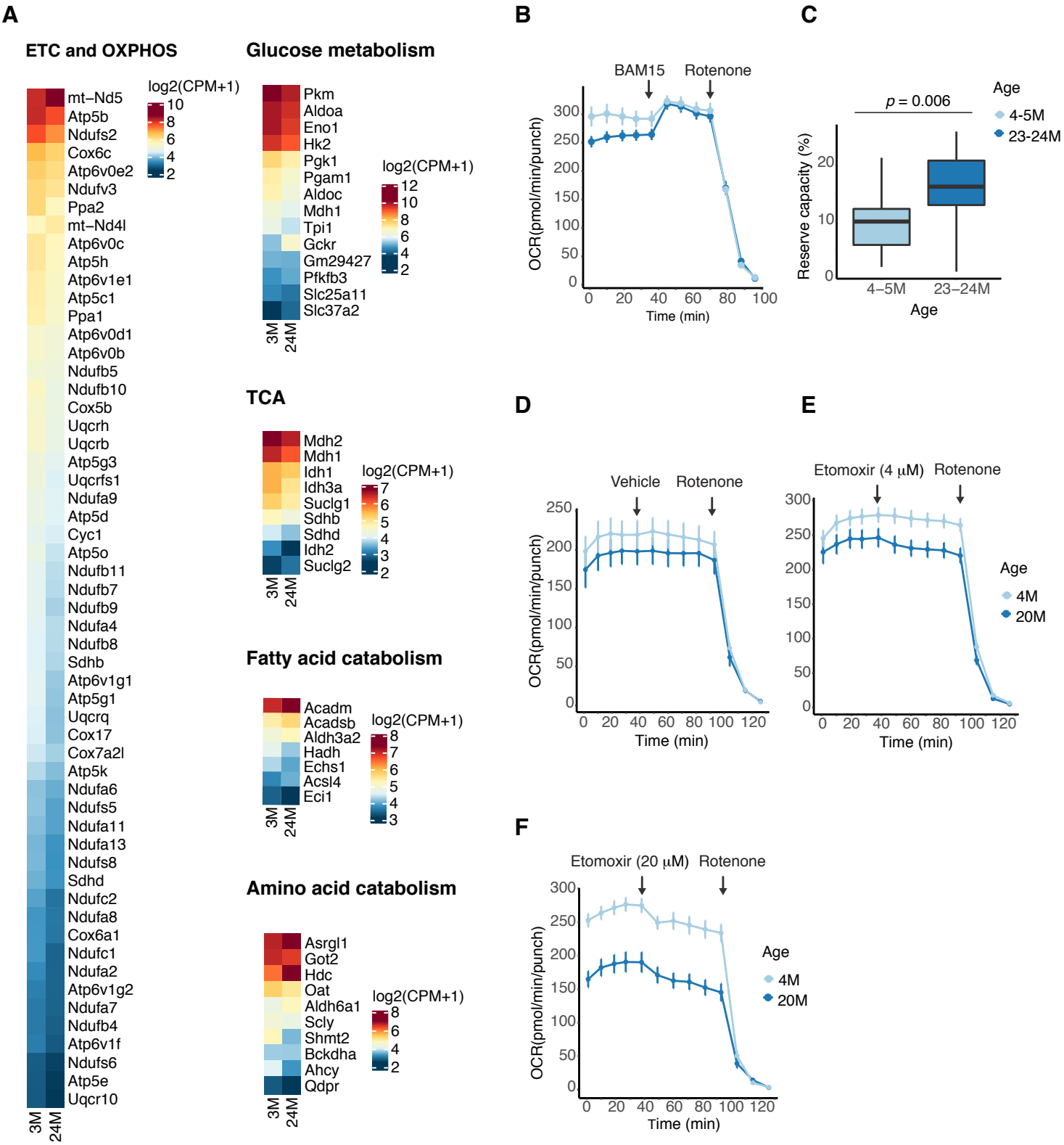

Figure S6. Alterations in energy metabolism with age. Related to figures 5 and 6. A) Heatmap of CPM (counts per million) transcript levels of genes involved in electron transport chain (ETC) and oxidative phosphorylation (OXPHOS), glycolysis, tricarboxylic acid (TCA) cycle, fatty acid catabolism, and amino acid catabolism. Absolute FC ≥ 1.2; FDR ≤ 0.1. B) OCR traces from young (4-5M) and old (23-24M) C57BL/6 wild-type mouse retinas. Arrows indicate the injection of a mitochondrial uncoupler (BAM15) or complex 1 inhibitor (rotenone) in the sample well. (C) A lower basal respiration and a larger mitochondrial reserve capacity can be observed in older mice as defined by 100*(maximal respiration-Basal respiration)/Maximal respiration. Error bars, +/- SEM. The mitochondrial reserve capacity in 4-5M vs 23-24M retina was compared by unpaired, two-sided t-test. D-F) OCR traces from young (4M) and old (20M) Nrlp-EGFP mouse retinas after addition of D) Vehicle (Ames buffer alone) or Etomoxir at E) 4 μM or F) 20 μM. Arrows indicate the injection of Etomoxir or rotenone in the sample well. OCR = oxygen consumption rate; BAM15 = (2-fluorophenyl)(6-[(2-fluorophenyl)amino](1,2,5-oxadiazolo[3,4-e]pyrazin-5-yl))amine.